

# FIBER AND VOID PROPERTY CORRELATION WITHIN BEAD MICROSTRUCTURE OF LARGE AREA ADDITIVE MANUFACTURING POLYMER COMPOSITES

Neshat Sayah and Douglas E. Smith\*

Department of Mechanical Engineering, Baylor University, Waco, TX, USA \*Corresponding author (douglas\_e\_smith@baylor.edu)

Keywords: Polymer Composite Extrusion Deposition, Fiber Orientation, Microstructural Voids

#### **ABSTRACT**

Short carbon fiber-reinforced polymer composites are widely employed in additive manufacturing (AM) techniques, including Large Area Additive Manufacturing (LAAM) polymer extursion-deposition, due to their superior mechanical properties compared to neat polymers. The mechanical and thermal properties of these composites are significantly influenced by factors such as fiber volume fraction, orientation, length, and distribution, and void distribution and volume fraction within the microstructure of the printed beads. This paper presents an experimental study that aims to quantitatively assess the relationship between void volume fraction and fiber orientation within the microstructure of both single freely extruded strands and single deposited beads of Short Carbon Fiber reinforced Acrylonitrile Butadiene Styrene (SCF/ABS) manufactured via a LAAM system. The study employs high-resolution 3D microcomputed tomography (µCT) to evaluate the fiber orientation, fiber volume fraction, and void volume fraction within the microstructure of the SCF/ABS composite parts. The findings demonstrate that the print direction  $A_{zz}$  component of the fiber orientation tensor in the regions near the edges of the single freely extruded strand is higher than those near the center, likely due to increased nozzle shear rate near the wall. Furthermore, within a single deposited bead on the print bed, the  $A_{zz}$  component varies throughout the microstructure. Measurements also show that regions with relatively higher void volume fraction have a corresponding lower fiber  $A_{zz}$  and fiber volume fraction for both the single freely extruded strand and the single deposited bead.

## 1 INTRODUCTION

Among several types of Additive Manufacturing (AM) methods, polymer composite extrusion-deposition is the most popular due to the availability of numerous neat thermoplastics and thermoplastic composite materials [1,2]. Polymer extrusion-deposition AM is performed on the small scale Fused Filament Fabrication (FFF) and on the large scale as Large Area Additive Manufacturing (LAAM), where the latter is the focus of this study. Short carbon fiber reinforced polymers are often employed in AM techniques due to their enhanced mechanical properties as compared with neat polymers. In these materials, the mechanical properties of the final part are highly dependent on properties fof the fiber suspension (i.e., fiber volume fraction, length, and orientation), as well as inter-bead voids and microstructural voids within the printed beads [3,4].

Inter-bead voids occur as a result of insufficient interlayer bonding during the FFF or LAAM fabrication process [4,5]. In addition, microstructural intra-bead voids develop within FFF and LAAM beads near the fibers due to the pressure distribution experienced by carbon fibers [6-8]. Furthermore, microstructural voids can also originate within the beads due to the entrapment of air during the manufacturing process or may stem from pre-existing voids present within the filaments or pellets prior to their use in the additive manufacturing process [5,9].

In polymer composites, the properties of the final product are influenced not only by the presence of voids within the microstructure but also by the orientation of fibers within the manufactured parts. To assess fiber orientation, Bay and Tucker calculated  $A_{ij}$  components of the fiber orientation tensor for a short fiber polymer composite, which commonly employed for evaluating the fiber orientation and alignment within the microstructure of polymer composites [10]. Additionally, previous research has focused on optimizing the printing process to control fiber alignment within the composite microstructure [3,11,12]. The majority of the investigations in the field have relied on two dimensional (2D) imaging techniques, such as electron microscopy, to assess the void content and fiber orientation within polymer composites. However, it is important to note that this technique introduces a potential bias due to its sectional nature, which can lead to errors in the analysis results. [13,14].

In recent years, µCT has garnered significant attention for its ability to provide high-resolution and high-quality three dimensional (3D) structural information. As a result, this technique has seen increased application in assessing fiber orientation and void volume fraction within additively manufactured polymer composites [13, 15, 16].

Unfortunately, there is still a lack of an established relationship between fiber orientation, fiber volume fraction, and void volume fraction within the microstructure of additively manufactured beads. This paper presents an experimental study with the objective of quantifying the relationship between key microstructural features, specifically fiber volume fraction, fiber orientation, and void volume fraction, utilizing  $\mu CT$  evaluation. The study focuses on investigating and reporting these relationships within both the single freely extruded strand and the single deposited bead manufactured via the LAAM system.

### 2 MATERIALS AND METHODS

## 2.1 3D Printing Process Parameters

Figure 1 shows the custom-built Baylor LAAM system used in this study that employs the Strangpresse Model 19 extruder (Strangpresse, Youngstown, OH, USA) [17], and includes a print volume of 48" x 48" x 6" [18]. The Model 19 single screw AM extruder has three temperature zones and a 3.172 mm diameter extrusion nozzle. PolyOne SCF/ABS pellets with 13% carbon fiber weight fraction (Avient Corporation, Avon Lake, OH, USA) were used as the LAAM feedstock. Prior to the 3D printing process, the pellets were dried in a convection oven and were left exposed to ambient room conditions which is expected to have increased the composite's moisture content prior to extrusion-deposition, leading to a higher than expected intra-bead void content (see results section below). This study includes LAAM extruder output as a freely extruded strand and a single deposited bead.

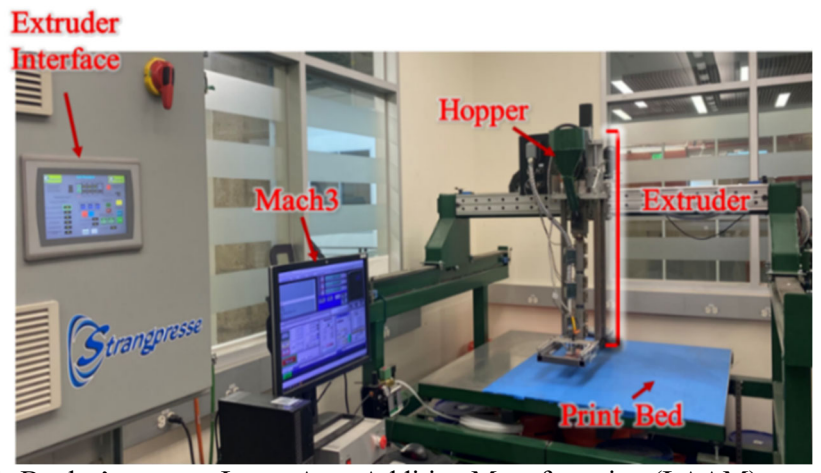


Figure 1. Baylor's custom Large Area Additive Manufacturing (LAAM) system [9]

To manufacture the single freely extruded strand, the nozzle height, defined as the distance between the nozzle tip and the aluminum print bed, was increased to 155 mm. Test samples were obtained by matching print speed to extrusion rate to prevent any elongation of the strand. Conversely, to create the single deposited bead, the extruder's nozzle height was set at 1.2 mm above the print surface. All 3D printing process parameters that were used to manufacture the single freely extruded strand and single deposited bead are shown in Table 1.

Printing Parameter	Value
Temperature	220 °C
Bead Nozzle Height	1.2 mm
Screw Speed	90 rpm

Table 1. LAAM SCF/ABS extrusion and deposition parameters

# 2.2 µCT Image Acquisition Technique

Micro-CT is a non-destructive technique utilized in this study to acquire comprehensive 3D microstructural information for our short fiber polymer composites, including details about the polymer matrix and carbon fiber reinforcements. An NSI X3000, X-RAY  $\mu$ CT system (North Star Imaging, Rogers, MN, USA) was employed to analyze the microstructure of both single freely extruded strands and single deposited beads. A resolution of 1.4 microns was set to detect the seven-micron diameter carbon fibers within the microstructure.  $\mu$ CT scans were then performed using an X-ray source at 60 kV and 900  $\mu$ A. Each sample underwent a 360-degree rotation in 1-degree increments, resulting in 2400 projections. The detector captured the transmitted X-ray signals, obtaining 2D attenuation distribution data. The acquired  $\mu$ CT scan data was reconstructed using efX-CT software (North Star Imaging, Minnesota, USA). Subsequently, the reconstructed data was imported into VGStudio Max 3.4 software (Volume Graphics GmbH, Heidelberg, Germany) for analysis of void volume fraction, fiber orientation, and fiber volume fraction within the microstructure of each sample. The VGDefX algorithm, integrated within the VGStudio Max porosity analysis module, was utilized for void analysis [9,19]. Additionally, fiber composite material analysis module was used to report the orientation tensor components and fiber volume fraction within the microstructure of each scanned part [20].

## **3 RESULTS AND DISCUSSIONS**

A typical 2D cross-section obtained from  $\mu$ CT scanning of the single freely extruded strand appears in Figure 2. The scan 3D dataset was divided into the five distinct regions of interest, as illustrated in Figure 2 to assess the spatial variability throughout the bead. VGStudio Max 3.4 was used to assess the diagonal components of the 2<sup>nd</sup> order fiber orientation tensor  $A_{xx}$ ,  $A_{yy}$ ,  $A_{zz}$  (see e.g., Bay and Tucker [10]), void volume fraction, and fiber volume fraction within each respective 3D region. The primary objective here is to conduct quantitative analysis to establish the relationship between these microstructural characteristics.

The variation of the diagonal components of the orientation tensor, void volume fraction, and fiber volume fraction within each sub-region is presented in Table 2. Note that the z-direction is the print direction which is normal to the plane of the image in Figure 2 such that  $A_{zz}$  represents the degree of alignment in the direction of the strand as it emerges from the nozzle. Table 2 shows that across all sub-regions in Figure 2, the  $A_{zz}$  component consistently exhibits the highest magnitude among the components of the orientation tensor. This observation shows that fibers align in the printing direction, as expected. Additionally, it is noteworthy that the  $A_{zz}$  components in regions near the edges (Regions 1 and 5, in Figure 2) are higher compared to regions near the center which is likely due to the higher nozzle shear rate near the wall.

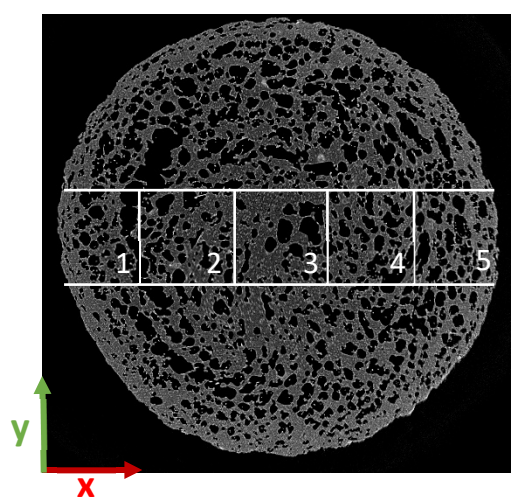


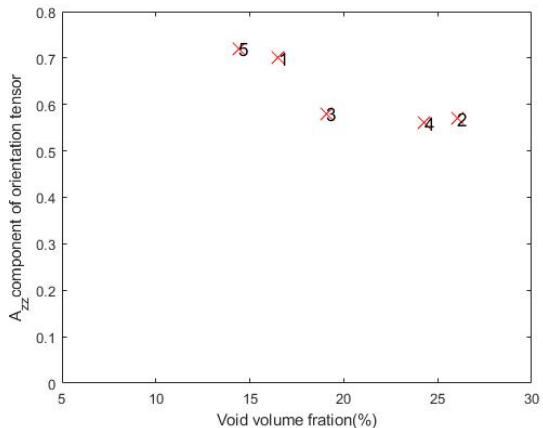
Figure 2. Typical μCT 2D view of single freely extruded strand divided into various regions of interest

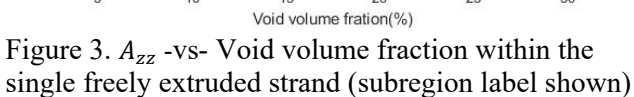
Region	$A_{\chi\chi}$	$A_{yy}$	$A_{zz}$	Void Volume Fraction (%)	Fiber Volume Fraction (%)
1	0.14	0.16	0.70	16.52%	10.12%
2	0.21	0.22	0.57	25.13%	7.37%
3	0.19	0.22	0.59	19.07%	9.89%
4	0.20	0.24	0.56	23.28%	8.13%
5	0.13	0.15	0.72	14.41%	10.26%

Table 2. Values of diagonal components of the orientation tensor, void volume fraction and fiber volume fraction within each sub-region within the single freely extruded strand

Figure 3 presents the relationship between the void volume fraction and the  $A_{zz}$  component of the orientation tensor for each sub-region in Figure 2. The results demonstrate that regions exhibiting a higher  $A_{zz}$  component, (indicating greater fiber alignment along the print direction), tend to have a reduced presence of micro voids. Furthermore, Figure 4. depicts the correlation between the fiber volume fraction and the  $A_{zz}$  component of the orientation tensor in different regions of the single freely extruded strand. The results reveal that regions characterized by a higher degree of fiber alignment along the print direction also exhibit a correspondingly higher void volume fraction. Note that void volume fraction is higher than expected here and in the single bead results below which is likely due to moisture content within the polymer feedstock. While this increase would likely not be as significant in production parts that followed a regimented drying process, its presence here provides a broader range of void volume fraction which aids in our understanding of the relationship between intra-bead voids and carbon fiber orientation and volume fraction.

Figure 5 illustrates the relationship between the void volume fraction and fiber volume fraction in the distinct sub-regions. The results demonstrate that an increase in the void volume fraction corresponds to a decrease in the fiber volume fraction within the various regions of interest. This finding highlights the inverse correlation between the void volume fraction and the presence of fibers within the analyzed regions.





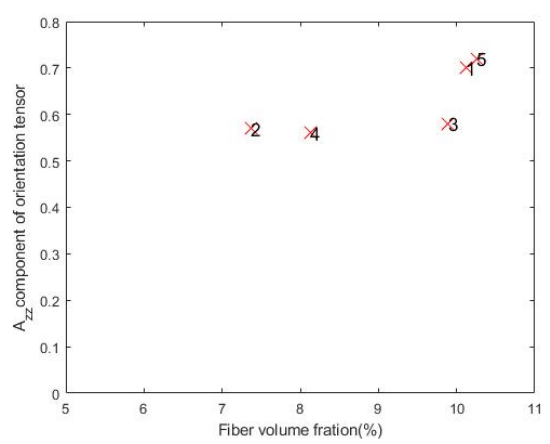


Figure 4.  $A_{zz}$  -vs- Fiber volume fraction within the single freely extruded strand (subregion label shown)

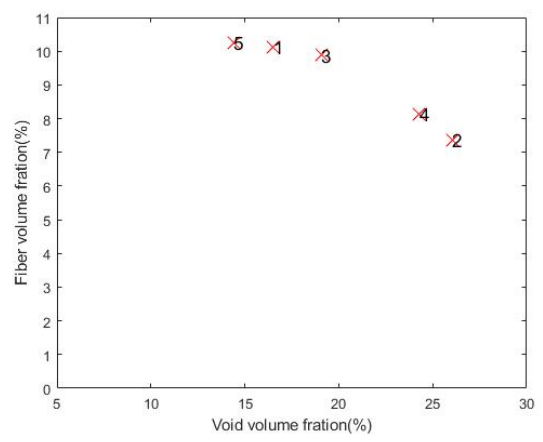


Figure 5. Fiber volume fraction-vs- Void volume fraction within the single freely extruded strand (subregion label shown)

A typical 2D cross-section obtained from  $\mu$ CT scanning of the single deposited bead appears in Figure 6. The 3D scanned sample was divided into nine distinct sub-regions of interest as shown in Figure 6 to provide a quantitative analysis and establish correlations between various microstructural features throughout the bead. Similar to the single freely extruded strand, the diagonal components of the 2<sup>nd</sup> order fiber orientation tensor ( $A_{xx}$ ,  $A_{yy}$ ,  $A_{zz}$ ), void volume fraction, and fiber volume fraction were evaluated within each of the nine regions of interest. Values of these diagonal components, in addition to void volume fraction, and fiber volume fraction within each sub-region appear in Table 3. Note that the  $A_{zz}$  component indicates the degree of carbon fiber alignment along the print direction, while  $A_{yy}$  indicates the amount of carbon fiber alignment normal to the print surface.

As shown in Table 3, a variation in microstructural features including fiber volume fraction and void volume fraction exist within different represented sub regions. Table 3 also presents compelling findings, indicating that the  $A_{zz}$  component is consistently highest among the various components of the orientation tensor across all sub-regions, as expected. This notable trend suggests the alignment tendency of the fibers along the printing process direction. Moreover, the results demonstrate a clear correlation between the increase in void volume fraction within a sub-region and a corresponding reduction in the  $A_{zz}$  component. Additionally, an increase in the void volume fraction is associated with a decrease in the fiber volume fraction within the microstructure.

Moreover, as indicated in Table 3, regions of interest near the center of the single deposited bead (regions 2 and 3 of Figure 6) have lower  $A_{zz}$  components than regions of interest near the edges (regions 7 and 9 of Figure. 6) which shows that higher degrees of fiber alignment near the edges is likely due to the higher nozzle shear rate near the nozzle wall.

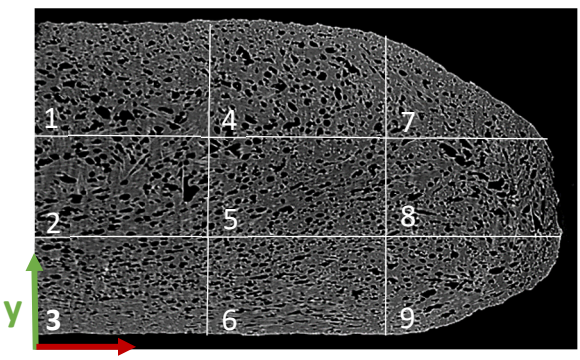


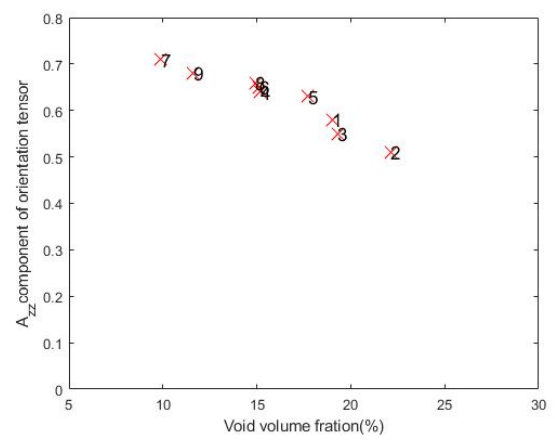
Figure 6. Typical μCT 2D view of single bead divided into various regions of interest

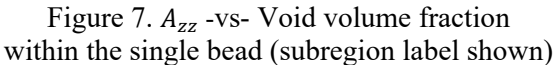
Region	$A_{xx}$	$A_{yy}$	$A_{zz}$	Void Volume Fraction (%)	Fiber Volume Fraction (%)
1	0.26	0.16	0.58	19.01%	7.28%
2	0.31	0.18	0.51	22.11%	6.19%
3	0.36	0.09	0.55	19.30%	6.33%
4	0.19	0.17	0.64	15.18%	8.72%
5	0.23	0.14	0.63	17.71%	8.38%
6	0.28	0.07	0.65	15.12%	8.92%
7	0.13	0.16	0.71	9.88%	10.21%
8	0.15	0.19	0.66	14.91%	9.56%
9	0.15	0.17	0.68	11.61%	10.15%

Table 3. Measured values of diagonal components of the orientation tensor, void volume fraction and fiber volume fraction within each sub-region within the single deposited bead

Figure 7 illustrates the correlation between the  $A_{zz}$  component and void volume fraction in subregions of the single deposited bead in Figure 6. The results reveal a consistent pattern, wherein regions with a higher void volume fraction exhibit a lower degree of fiber alignment along the print direction (lower  $A_{zz}$  values). Figure 8. presents the relationship between the  $A_{zz}$  component of the orientation tensor and fiber volume fraction within the microstructure of the single deposited bead. The results demonstrate that subregions with a higher fiber volume fraction exhibit a greater degree of fiber alignment along the print direction, indicating a negative correlation between fiber alignment and void volume fraction.

Furthermore, as highlighted in Table 3, the regions closer to the center of the single deposited bead (region 2 and region 3 in Figure 6) exhibit lower  $A_{zz}$  components compared to the regions near the edges (region 7 and region 9 in Figure 6). The higher degree of fiber alignment observed near the edge is likely due to the higher shear rate near the nozzle wall.





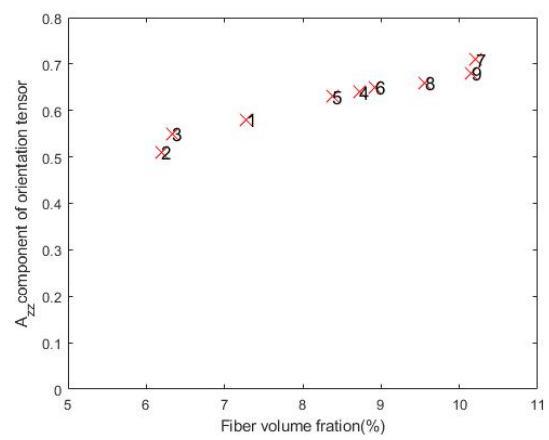


Figure 8.  $A_{zz}$  -vs- Fiber volume fraction within the single bead (subregion label shown)

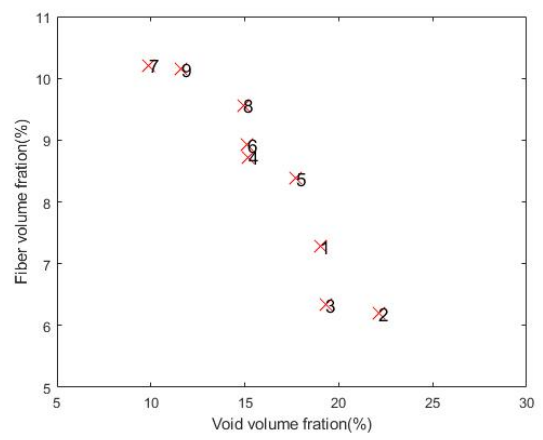


Figure 9. Fiber volume fraction-vs- Void volume fraction within the single bead (subregion label shown)

## **4 CONCLUSIONS**

This study aims to quantitatively assess the relationship between the void volume fraction and fiber orientation and volume fraction within the microstructure of single freely extruded strand and the single deposited bead of SCF/ABS manufactured via the LAAM system, employing  $\mu$ CT measurements and analyses. In order to gain a better understanding of the interaction between these microstructural features, the 3D samples obtained for a single freely extruded strand and a single deposited bead were subdivided into regions of interest. The results consistently demonstrate that the  $A_{zz}$  component exhibits the highest magnitude among the components of the orientation tensor across all regions. This finding suggests a strong tendency for the fibers to align with the extrusion direction within the single freely extruded strand as expected. Moreover, within the microstructure of the single deposited bead, the fibers tend to be oriented along the print direction.

Measured results obtained in this study reveal a consistent and significant pattern among the microstructural features of interest. In regions characterized by a higher void volume fraction, there is a corresponding decrease in the degree of fiber alignment along the extrusion and print directions, as indicated by lower  $A_{zz}$  values. This observation provides empirical evidence supporting a negative relationship between  $A_{zz}$  and void volume fraction within the respective subregions. Furthermore, the results

demonstrate that subregions with a higher fiber volume fraction exhibit a heightened degree of fiber alignment along the print and extrusion directions, suggesting a positive correlation between fiber alignment and void volume fraction. Furthermore, the results indicate that within the single deposited bead, subregions located near the center of the bead exhibit lower values of the  $A_{zz}$  component, whereas higher values are observed in the regions near the edge. This observation is likely attributable to the elevated shear rate existed at the nozzle wall.

## **ACKNOWLEGMENTS**

The authors would like to express their gratitude to the US National Science Foundation (grant #2055628) for their financial support, and to Strangpresse for providing the Model 19 extruder used in this study.

### REFERENCES

- [1] T. Mulholl, S. Goris, J. Boxleitner, T.A. Osswald, and N. Rudolph, "Process-induced fiber orientation in fused filament fabrication". Journal of Composites Science, 2(3), p.45, 2018.
- [2] K.M.M. Billah, F.A. Lorenzana, N.L. Martinez, R.B. Wicker and D.Espalin. "Thermomechanical characterization of short carbon fiber and short glass fiber-reinforced ABS used in large format additive manufacturing". Additive Manufacturing, 35, p.101299, 2020.
- [3] D. Yang, H. Zhang, J. Wu, and E.D. McCarthy. "Fibre flow and void formation in 3D printing of short fibre reinforced thermoplastic composites: an experimental mark exercise". Additive Manufacturing, 37, p.101686, 2021.
- [4] H.L. Tekinalp, V. Kunc, G.M. Velez-Garcia, C.E. Duty, L.J. Love., A.K. Naskar, C.A. Blue, and S. Ozcan. "Highly oriented carbon fiber–polymer composites via additive manufacturing". Composites Science and Technology, 105, pp.144–150, 2014.
- [5] Sosa-Rey, F., Abderrafai, Y., Lewis, A.D., Therriault, D., Piccirelli, N. and Lévesque, M., 2022. OpenFiberSeg: Open-source segmentation of individual fibers and porosity in tomographic scans of additively manufactured short fiber reinforced composites. Composites Science and Technology, 226, p.109497.
- [6] Wang, Z., Fang, Z., Xie, Z. and Smith, D.E., 2022. A Review on Microstructural Formations of Discontinuous Fiber-Reinforced Polymer Composites Prepared via Material Extrusion Additive Manufacturing: Fiber Orientation, Fiber Attrition, and Micro-Voids Distribution. Polymers, 14(22), p.4941.
- [7] Awenlimobor, A., Smith, D.E., Wang, Z. and Luo, C., 2022. Three-dimensional (3D) Simulation of Micro-Void Development within Large Scale Polymer Composite Deposition Beads. In 2022 International Solid Freeform Fabrication Symposium.
- [8] Awenlimobor, A., Wang, Z. and Smith, D.E., 2021. Physical Modeling: Simulation of Micro-Void Development within Large Scale Polymer Composite Deposition Beads. In 2021 International Solid Freeform Fabrication Symposium. University of Texas at Austin.
- [9] Sayah, N. and Smith, D.E., 2022. Effect of Process Parameters on Void Distribution, Volume Fraction, and Sphericity within the Bead Microstructure of Large-Area Additive Manufacturing Polymer Composites. Polymers, 14(23), p.5107.
- [10] Bay, R.S. and Tucker III, C.L., 1992. Stereological measurement and error estimates for three-dimensional fiber orientation. Polymer Engineering & Science, 32(4), pp.240-253.
- [11] Lewicki, J.P., Rodriguez, J.N., Zhu, C., Worsley, M.A., Wu, A.S., Kanarska, Y., Horn, J.D., Duoss, E.B., Ortega, J.M., Elmer, W. and Hensleigh, R., 2017. 3D-printing of meso-structurally ordered carbon fiber/polymer composites with unprecedented orthotropic physical properties. Scientific reports, 7(1), p.43401.
- [12] Tseng, P., Napier, B., Zhao, S., Mitropoulos, A.N., Applegate, M.B., Marelli, B., Kaplan, D.L. and Omenetto, F.G., 2017. Directed assembly of bio-inspired hierarchical materials with controlled nanofibrillar architectures. Nature nanotechnology, 12(5), pp.474-480.
- [13] Sommacal, S., Matschinski, A., Drechsler, K. and Compston, P., 2021. Characterisation of void and fiber distribution in 3D printed carbon-fiber/PEEK using X-ray computed tomography. Composites Part A: Applied Science and Manufacturing, 149, p.106487.
- [14] Garcea, S.C., Wang, Y. and Withers, P.J., 2018. X-ray computed tomography of polymer composites. Composites Science and Technology, 156, pp.305-319.

- [15] Diouf-Lewis, A., Farahani, R.D., Iervolino, F., Pierre, J., Abderrafai, Y., Lévesque, M., Piccirelli, N. and Therriault, D., 2022. Design and characterization of carbon fiber-reinforced PEEK/PEI blends for Fused Filament Fabrication additive manufacturing. *Materials Today Communications*, 31, p.103445.
- [16] Dana, H.R., Barbe, F., Delbreilh, L., Azzouna, M.B., Guillet, A. and Breteau, T., 2019. Polymer additive manufacturing of ABS structure: Influence of printing direction on mechanical properties. *Journal of Manufacturing Processes*, 44, pp.288-298.
- [17] https://pitchbook.com/profiles/company/187809-94
- [18] Russell, T.D., 2017. The effects of fiber orientation on stiffness and thermal expansion of large volume, anisotropic, short-fiber, composite material fabricated by Fused Filament Fabrication (Doctoral dissertation).
- [19] Wang, X., Zhao, L., Fuh, J.Y.H. and Lee, H.P., 2019. Effect of porosity on mechanical properties of 3D printed polymers: Experiments and micromechanical modeling based on X-ray computed tomography analysis. Polymers, 11(7), p.1154.
- [20] https://www.volumegraphics.com/en/products/vgsm/fiber-composite-material-analysis